

# Certified Zeroth-order Black-Box Defense with Robust UNet Denoiser

Astha Verma  
IIIT Delhi  
asthav@iiitd.ac.in

Siddhesh Bangar  
MIDAS LAB, IIIT Delhi  
siddheshb008@gmail.com

A V Subramanyam  
IIIT Delhi  
subramanyam@iiitd.ac.in

Naman Lal  
MIDAS LAB, IIIT Delhi  
namanlal.lal92@gmail.com

Rajiv Ratn Shah  
IIIT Delhi  
rajivrtn@iiitd.ac.in

Shin'ichi Satoh  
NII Tokyo  
satoh@nii.ac.jp

## Abstract

*Certified defense methods against adversarial perturbations have been recently investigated in the black-box setting with a zeroth-order (ZO) perspective. However, these methods suffer from high model variance with low performance on high-dimensional datasets due to the ineffective design of the denoiser and are limited in their utilization of ZO techniques. To this end, we propose a certified ZO preprocessing technique for removing adversarial perturbations from the attacked image in the black-box setting using only model queries. We propose a robust UNet denoiser (RDUNet) that ensures the robustness of black-box models trained on high-dimensional datasets. We propose a novel black-box denoised smoothing (DS) defense mechanism, ZO-RUDS, by prepending our RDUNet to the black-box model, ensuring black-box defense. We further propose ZO-AE-RUDS in which RDUNet followed by autoencoder (AE) is prepended to the black-box model. We perform extensive experiments on four classification datasets, CIFAR-10, CIFAR-100, Tiny Imagenet, STL-10, and the MNIST dataset for image reconstruction tasks. Our proposed defense methods ZO-RUDS and ZO-AE-RUDS beat SOTA with a huge margin of 35% and 9%, for low dimensional (CIFAR-10) and with a margin of 20.61% and 23.51% for high-dimensional (STL-10) datasets, respectively.*

## 1. Introduction

A notable amount of success has been attained by machine learning (ML) models [37, 39], and deep neural networks (DNNs) in particular because of their better predictive capabilities. However, their lack of robustness and susceptibility to adversarial perturbations has caused serious worries about their wide-scale adaptation in a number of artificial intelligence (AI) applications [26, 11, 55, 7, 23, 4]. These adversarial attacks have motivated vari-

ous strategies to strengthen ML models as a key area of research [53, 5, 78, 19]. Among these techniques, adversarial training (AT) [65, 53] is one of the prominent defense strategies. The advancements AT led to various empirical defense methods [6, 70, 75, 13, 78], however these methods may not always be certifiably robust [69, 18]. Another line of research is certified defense, where an off-the-shelf model's prediction is certified within the neighborhood of the input. These methods are called certified defense techniques [74, 57, 38, 61, 62, 60].

Cohen *et al.* [17] first proposed randomized smoothing (RS), which certifies defense by forming a smoothed model from the empirical model by adding Gaussian noise to the input images. Few other works have been proposed which provide certified defense inspired by randomized smoothing [62, 60, 2]. Salman *et al.* [62] pre-pended a custom-trained denoiser to the predictor for increased robustness. In another work, Salman *et al.* [60] apply visual transformers within the smoothing network in order to provide certified robustness to adversarial patches. While previous works in adversarial defense have achieved promising advancements, robustness is provided over white-box models with known architectures and parameters. The white-box assumption, however, has high computational complexity as models are trained end-to-end as in AT, thus limiting the practicality and scalability of the defense method. For instance, it becomes impractical to retrain complex ML models trained on a vast number of MRIs or CT scans [64, 33].

Moreover, privacy concerns may arise when implementing white-box defense since the owner may not wish to reveal model information. This is because attacks such as membership inference and model inversion attacks expose the vulnerabilities of the training data [25]. Due to the scalability and privacy issues, few previous works tackled the highly non-trivial problem of adversarial defense in the black-box setting ('black-box defense') [62, 81].

Salman *et al.* [62] used surrogate models as approxi-

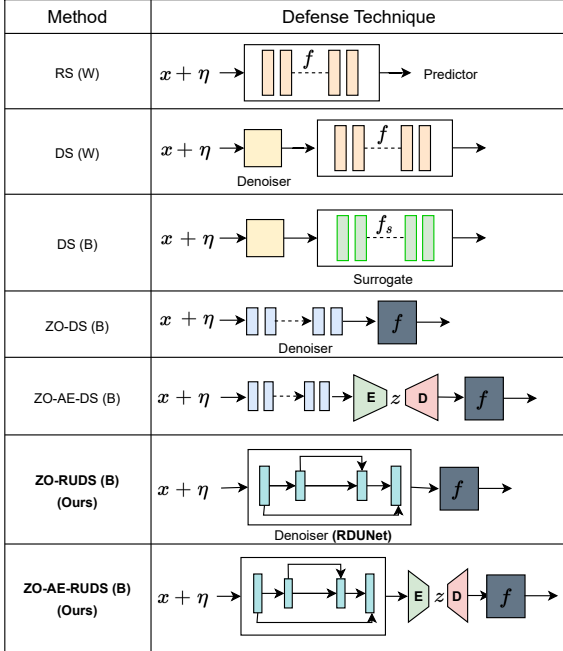


Figure 1: We make a comparison with four previous certified defense methods, including RS [17], DS (W) [62], DS (B) [62], ZO-DS [81] and ZO-AE-DS [81] (ZO-optimization approaches). ‘W’ and ‘B’ refer to white-box (defense technique can utilize weights of target model  $f$ ) and black-box settings. ‘ $x$ ’ - input sample, ‘ $\eta$ ’ - noise, ‘E’ - Encoder, ‘D’ - Decoder, ‘ $f$ ’ - target model, ‘ $f_s$ ’ - surrogate model (proxy of  $f$ ), and ‘ $z$ ’ - latent feature vector.

mates of the black-box models, over which defense may be done using the white-box setup. However, this setup requires information on the target model type and its function, which may be not be available practically. In another recent work, Zhang *et al.* [81] proposed a more authentic black-box defense of DNN models with the help of the zeroth-order optimization perspective. They pre-pended a custom-trained denoiser as in [62] followed by an autoencoder architecture to the target model and trained it with ZO optimization. However, [81] fails to perform for high dimensional datasets like Tiny imagenet with the dimensionality of  $299 \times 299 \times 3$  as the denoiser used may fail to preserve spatial information. The main contribution of [81], that is, the addition of autoencoder to existing technique [62], enhances the robustness of black-box model to some extent for low-dimensional datasets like CIFAR-10 ( $32 \times 32 \times 3$ ). However, this limits its usage to only the coordinate-wise gradient estimation (CGE) ZO optimization technique. However, our proposed approach can utilize two main existing ZO optimization techniques: randomized gradient estimate (RGE) and CGE. We discuss in detail in subsection 5.2, where we prove the limitations of [81] on

high dimensional datasets graphically.

We propose a certified black-box defense ZO-RUDS using the ZO optimization technique, where we pre-pend a novel robust UNet denoiser (RDUNet) to the target model. We further pre-pend our RDUNet and custom-trained autoencoder and propose the ZO-AE-RUDS defense mechanism. Our proposed methods require only input queries and output feedback and provide defense in a pure black-box setting. Unlike SOTA [81], which leads to high model variance on direct application of ZO optimization on the custom-trained denoiser, our proposed RDUNet, due to its architectural advantage over previous denoisers decreases model variance and provides better performance with direct application of ZO optimization. We experiment with various denoisers and prove that our RDUNet denoiser provides improved performance for both low-dimensional and high-dimensional datasets. Since we are dealing with a difficult ZO optimization and cannot back-propagate through the model, we optimize our proposed model by utilizing the black-box model’s predicted labels and softmax probabilities. In order to further increase the certification of our proposed approach, we utilize maximum mean discrepancy (MMD) to bring the distributions of original input images closer to obtained denoised output. We provide an illustration of certified defense techniques and compare them to our approach in Figure 1.

We summarize our contributions as follows:

- We propose a certified black-box defense mechanism based on the preprocessing technique of pre-pending a robust denoiser to the predictor to remove adversarial noise using only the input queries and the feedback obtained from the model.
- We design a novel robust UNet denoiser RDUNet which defends a black-box model with ZO optimization approaches. Unlike previous ZO optimization-based defense approaches, which give a poor performance on high-dimensional data due to high model variance, our UNet-based robustification model gives high performance for both low-dimensional and high-dimensional datasets.
- We conduct extensive experiments and show that our proposed defense mechanism beats SOTA by a huge margin on four classification datasets, CIFAR-10, CIFAR-100, STL-10, Tiny Imagenet, and on MNIST dataset for reconstruction task.

## 2. Related Work

We broadly categorize the literature on robust defense into empirical and certified defense and briefly discuss them below in the white-box and black-box settings.

## 2.1. Empirical Defense

Szegdy *et al.* [65] first proposed robust empirical defense in the form of adversarial training (AT). Due to AT, there has been a rapid increase in empirical defense methods [70, 75, 15, 71, 13]. Zhang *et al.* [78] proposed a tradeoff between robustness and accuracy that can optimize defense performance. In order to improve the scalability of AT, empirical robustness is provided by previous works which design computationally light alternatives of AT [12, 63]. Some recent empirical defense works are based on the concept of distillation, initially proposed by Hinton *et al.* [29]. Papernot *et al.* [56] presented a defensive distillation strategy to counter adversarial attacks. Folz *et al.* [24] gave a distillation model for the original model, which is trained using a distillation algorithm. It masks the model gradient in order to prevent adversarial perturbations from attacking the model’s gradient information. Addepalli *et al.* [1] proposed unique bit plane feature consistency (BPFC) regularizer to increase the model’s resistance to adversarial attacks.

## 2.2. Certified Defense

Unlike empirical defense, the certified defense provides formal verification of robustness of the DNN model [52, 28, 22]. Certified robustness is given by a ‘safe’ neighbourhood region around the input sample where the prediction of DNN remains same. Previous works [38, 67, 8, 21] in this field provide ‘exact’ certification, which is often computationally intensive and is not scalable to large architectures. Katz *et al.* [38] proposed a robust simplex verification method to handle non-linear ReLU activation functions. Another line of work [74, 77], which provides ‘incomplete’ verification, requires less computation; however, it gives faulty certification and can decline certification even in the absence of adversarial perturbation. Both ‘exact’ and ‘incomplete’ posthoc certification methods require customized architectures and hence are not suitable for DNNs [81].

Another area of study focuses on in-process certification-aware training and prediction. For instance, a randomized smoothing (RS) convolves an empirical classifier with an isotropic Gaussian distribution to convert it into a provably reliable one. In [17], it was demonstrated that RS could offer formal assurances for adversarial robustness. As well as, there are several different RS-oriented verifiable defences that have been developed, including adversarial smoothing [61], denoised smoothing [62], smoothed ViT [60], and feature smoothing [2].

## 2.3. ZO Optimization for adversarial learning.

ZO optimization is useful in solving black-box problems where gradients are difficult to compute or infeasible to obtain [76, 72]. These methods are gradient-free counterparts of first-order (FO) optimization methods [48]. Recently, ZO

optimization has been used for generating adversarial perturbations in black-box setting [14, 35, 34, 68, 47, 50, 32, 9, 10]. Similar to attack methods, ZO optimization can also be applied to black-box defense methods with access only to the inputs and outputs of the targeted model. Zhang *et al.* [81] proposed black-box defense using ZO optimization and leveraged autoencoder architecture for optimizing the defense approach with CGE optimization. However, their approach fails to perform for high-dimension datasets. Inspired from [81], we propose a better defense mechanism with a robust UNet denoiser which gives high performance for high-dimension images.

## 3. Preliminaries

**Notations and Basics.** Let  $x \in \mathbb{R}^d$  is the input sample and  $l \in \{1, 2, \dots, \mathbb{Y}\}$  be the label. An adversarial attack can perturb  $x$  by adding an adversarial noise. In order to defend model  $f$  against these adversarial attacks and to provide certified robustness, [17] proposed randomized smoothing (RS), a technique to construct a smoothed classifier  $f_s$  from  $f$ . It is given as,

$$f_s(x) = \arg \max_{l \in \mathbb{Y}} \mathbb{P}_{\eta \in N(0, \sigma^2 I)} [f(x + \eta) = l], \quad (1)$$

where  $\eta$  is the Gaussian noise with standard deviation  $\sigma$ .

**Randomized Smoothing and Certified Robustness.** [44] and [45] first gave robustness guarantees for the smoothed classifier  $f_s$  using RS, but it was loosely bounded. [17] proposed a tight bound on  $l_2$  robustness guarantee for the smoothed classifier  $f_s$ . They used Monte Carlo sampling and proposed an effective statistical formulation for predicting and certifying  $f_s$ . If the prediction of the base classifier for noise perturbed input samples ( $x + \eta$ ) is the probability  $p_f$  as the topmost prediction, and  $p_s$  is the runner-up prediction. Then the smoothed classifier is robust within the radius  $R_c$  assuming that  $f_s$  gives correct prediction.  $R_c$  is the certified radius within which the predictions are guaranteed to remain constant. [17] gave lower and upper bound estimates for  $p_f$  and  $p_s$  as  $\underline{p}_f$  and  $\overline{p}_s$  respectively using Monte Carlo technique.

**Theorem 1 ([17])** *Given  $f$  is the base classifier which returns the target label of the input sample, and  $f_s$  is the smoothed classifier, then assuming that  $f_s$  classifies correctly, the probabilities of topmost and runner-up predictions are given as:*

$$p_f = \max \mathbb{P}_\eta [f(x + \eta) = l] \quad (2)$$

$$p_s = \max_{l' \neq l} \mathbb{P}_\eta [f(x + \eta) = l'], \quad (3)$$

where  $\eta$  is the noise sampled from the Gaussian distribution  $N(0, \sigma^2)$ . Then,  $f_s$  is robust inside a radius  $R_c$ , which is given as:

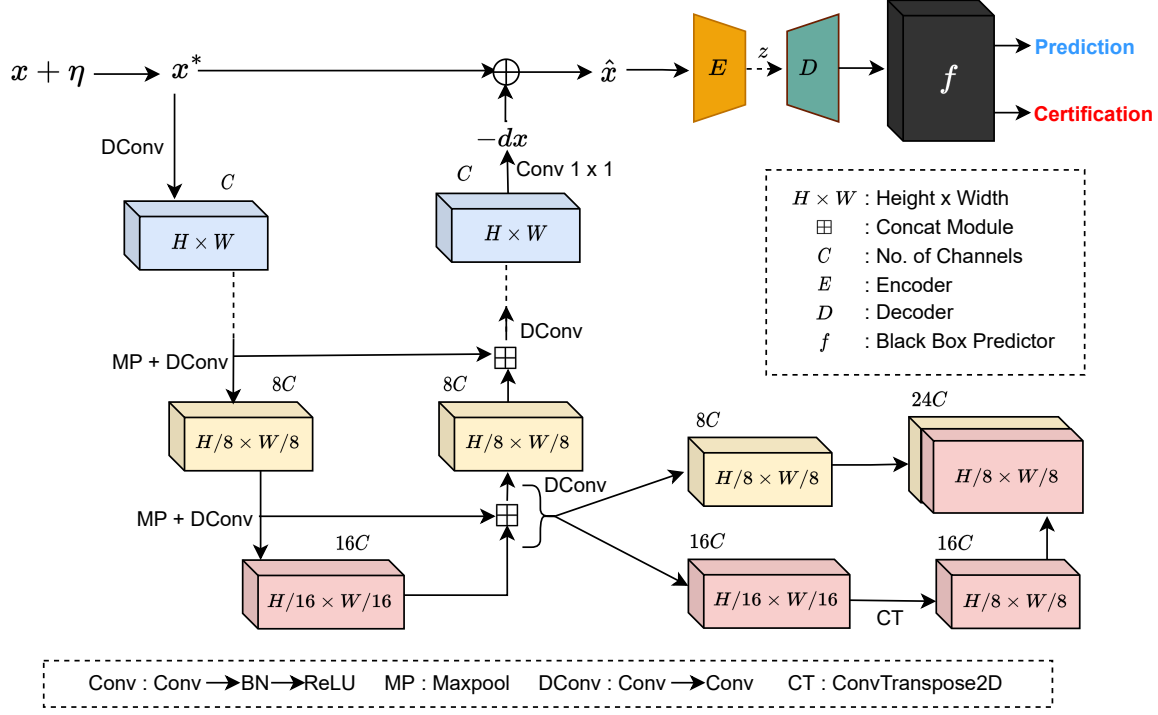


Figure 2: An overview of proposed certified defense mechanism via robust UNet denoiser RDUNet. Noise  $\eta$  is added to input sample  $x$  which is given as input to the robust denoiser. The output of denoiser is the residual map which when added to noisy image  $x^*$  gives denoised output  $\hat{x}$ . The denoised output is input of the autoencoder architecture which is then send as input to black-box model  $f$ .

$$R_c = \frac{\sigma}{2} [\phi^{-1}(p_f) - \phi^{-1}(p_s)], \quad (4)$$

where  $\phi^{-1}$  is the inverse of standard Gaussian CDF. If  $p_f$  and  $p_s$  hold the below inequality:

$$p_f \geq \underline{p}_f \geq \overline{p}_s \geq p_s \quad (5)$$

Then,  $R_c$  is given as:

$$R_c = \frac{\sigma}{2} [\phi^{-1}(\underline{p}_f) - \phi^{-1}(\overline{p}_s)] \quad (6)$$

The enhancement of the smoothed classifier’s robustness relies on the application of the “Neyman-Pearson” lemma, which is used to derive the above expressions [17].

**Denoised Smoothing (DS).** [62] proposed that naively applying randomized smoothing gives low robustness, as the standard classifiers are not trained to be robust to the Gaussian perturbation of the input sample. ‘DS’ augments a custom-trained denoiser  $D_\theta$  to base classifier  $f$ . In this approach, an image-denoising pre-processing step is employed before input samples are passed through  $f$ . The denoiser pre-pended smoothed classifier, which is effective at

removing the Gaussian noise, is given as,

$$f_s(x) = \arg \max_{l \in \mathbb{Y}} \mathbb{P}_{\eta \in N(0, \sigma^2 I)} [f(D_s^\theta(x + \eta)) = l]. \quad (7)$$

In order to obtain the optimal denoiser  $D_s^\theta$ , DS proposed a stability regularized denoising loss in the first-order optimization setting. It is given as,

$$\begin{aligned} \mathcal{L}_{MSE+STAB}(\theta) = & \mathbb{E}_{T, \eta} \|D_s^\theta(x + \eta) - x\|_2^2 \\ & + \mathbb{E}_{T, \eta} [\mathcal{L}_{CE}(f(D_s^\theta(x + \eta)), f(x))], \end{aligned} \quad (8)$$

where  $T$  is the training dataset and  $\mathcal{L}_{CE}$  is the cross-entropy loss. However, previous approaches provide certified robustness in white-box setting with access to the target model’s architectures and parameters. [62] first proposed certified defense in black-box setting. However, they utilized surrogate model which requires the information about model type and its function. Recently, [81] proposed certified black-box defense with ZO optimization.

## 4. Methodology

In this section, we first describe the architecture of our proposed robust defense model. We then describe the objective function of our proposed defense mechanism. Lastly, we discuss our two proposed defense mechanisms using RGE and CGE ZO optimization approaches. Our proposed framework is as shown in Figure 2.

**Problem Statement.** We aim to defend a black-box model  $f$ , where  $f$  is used for classification or reconstruction purposes. We consider  $l_2$  norm-ball constrained adversarial attacks as our threat [26].

**Notations.** We consider input samples as  $x$  and  $l \in \{1, 2, \dots, L\}$  be the predicted label. Noise and noise-perturbed images are represented as  $\eta$  and  $x^*$ , respectively. We denote our proposed learnable RDUNet as  $D_\theta^u$ . We denote encoder and decoder as  $E_{\theta_e}$  and  $D_{\theta_d}$  respectively. We represent our black-box predictor as  $f$ . We denote RGE and CGE ZO optimization as R and C, respectively.

### 4.1. Proposed Robust Architecture

We provide a robust black-box defense by pre-pending our proposed robust denoiser RDUNet, followed by a custom-trained AE to the black-box predictor. We show the architecture of our proposed RDUNet in Figure 2. The network has a feedforward and a feedback path. We have a stack of conv layers, and each conv layer contains a convolution layer with kernel size  $3 \times 3$  and padding of 1, followed by batch normalization layer [36] and rectified linear unit [42]. DConv represents two consecutive conv layers. Our feedforward path consists of five blocks: one is DConv block, and four are Maxpooling + DConv.

RDUNet has four blocks with a fusion module followed by DConv operation in the feedback path. The last block in the feedback path is a convolution layer with kernel size  $1 \times 1$ . Fusion module receives two inputs, one feedback input from the feedback path and the lateral input from the feedforward path. We use ConvTranspose2D [20] to upsample the feedback input to the same size as the lateral input. The feedforward path generates feature maps of increasingly lower resolutions, and along the feedback path, the feature maps have an increasingly higher resolution, as is visible from Figure 2. The denoised output  $\hat{x}$  is the sum of noisy image  $x^*$  and  $-d\hat{x}$ . It is represented as,  $\hat{x} = x^* + (-d\hat{x})$ .

### 4.2. Proposed Objective Function

Our proposed robustification model is trained by using different losses designed for ensuring three objectives, (i) correct predictions by  $f$  on the denoised output  $\hat{x}$ , (ii) the similarity between the features of clean training samples  $x$  and denoised output  $D_\theta^u(x^*)$ , and (iii) decrease in the domain gap between the probability distributions of clean

samples and denoised output.

**Robust Prediction.** We use cross-entropy loss  $\mathcal{L}_{CE}$  [83] to make sure that the label predicted by the black-box model of the original input sample is same as that of the denoised output of its Gaussian-perturbed counterpart.

$$\mathcal{L}_{CE}(\theta) = \mathbb{E}[-p(f(x)^l) \log(p(f(D_\theta^u(x^*))^l))], \quad (9)$$

where  $f(x)$  is a black-box predictor which takes an input  $x$  and makes a predictions.  $p(f(x)^l)$  and  $p(f(D_\theta^u(x^*))^l)$  are the probabilities predicted by  $f$  for clean samples and denoised output.

**Feature Similarity.** We leverage the information that the black-box model trained on the training dataset is highly discriminative. Thus, we propose cosine similarity to learn a mapping between the logit features of the original input images ( $f(x)$ ) and the logits of the output obtained from the denoiser of the Gaussian perturbed inputs ( $f(D_\theta^u(x^*))$ ).

$$\mathcal{L}_{CS}(\theta) = \mathbb{E}\left[\frac{f(x)^\top f(D_\theta^u(x^*))}{\|f(x)\| \|f(D_\theta^u(x^*))\|}\right]. \quad (10)$$

**Domain Similarity.** In addition to maintaining the label and feature consistency at the sample level, we want to bring the domain distribution of synthesized denoised images closer to the original input sample by using maximum mean discrepancy ( $MMD(\mu, v)$ ) [27] on the features of input images ( $f_{feat}(x)$ ) and features of denoised output ( $f_{feat}(D_\theta^u(x^*))$ ). This distribution pulling of the original samples and denoised output is inspired by the task of domain adaptation [54, 80].

$$\mathcal{L}_{MMD}(\theta) = MMD(f_{feat}(x), f_{feat}(D_\theta^u(x^*))). \quad (11)$$

**Our Overall Objective Function.** We optimize our certified defense mechanism with loss functions given in Eq. 9, 10 and 11

$$\mathcal{L}_{Tot}(\theta) = \mathcal{L}_{CE} + \lambda_{CS}\mathcal{L}_{CS} + \lambda_{MMD}\mathcal{L}_{MMD}, \quad (12)$$

where  $\lambda_{CS}$  and  $\lambda_{MMD}$  are the weights assigned to the loss functions. However, since we cannot access the parameters or weights of the model, we cannot optimize our model using standard optimizers like SGD [3] or ADAM [82] as that would require back-propagation through the predictor. Thus, we utilize ZO optimization approaches where values of functions are approximated instead of using true gradients.

### 4.3. Proposed Black-Box Defense Methods

We discuss in this section our two defense methods in detail:

**ZO Robust UNet Denoised Smoothing (ZO-RUDS) Defense (RGE Optimization).** In order to achieve ZO-RUDS

with our proposed pre-pended RDUNet denoiser to the black-box model  $f$ , we represent our objective function as,

$$\mathcal{L}_{Tot}^R(\theta) := \mathcal{L}_{Tot}(f(D_\theta^u(x^*)), \quad (13)$$

where  $\mathcal{L}_{Tot}^R(\theta)$  represents that we optimize  $\mathcal{L}_{Tot}$  (Eq. 12) with RGE ZO optimization (R) [48]. We calculate gradient estimate of  $\mathcal{L}_{Tot}^R(\theta)$  as,

$$\hat{\nabla}_\theta \mathcal{L}_{Tot}^R(\theta) \approx \frac{dD_\theta^u(x^*)}{d\theta} \hat{\nabla}_z f(z)|_{z=D_\theta^u(x^*)}, \quad (14)$$

where  $\hat{\nabla}_z f(z)$  is the ZO gradient estimate of  $f$ . We calculate the RGE ZO gradient estimate of  $\mathcal{L}_{Tot}^R(\theta)$  by the difference of two function values along a set of random direction vectors. It is represented as:

$$\hat{\nabla}_\theta \mathcal{L}_{Tot}^R(\theta) = \sum_{k=0}^{q-1} \left[ \frac{d}{\xi \cdot q} (\mathcal{L}_{Tot}(\theta + \xi u_k) - \mathcal{L}_{Tot}(\theta)) u_k \right], \quad (15)$$

$q$  are the querying directions, and  $u \in \{1, 2, \dots, q\}$  are  $q$  independently and uniformly drawn random vectors from a unit Euclidean sphere  $\xi > 0$  is the smoothing parameter with a small step size of 0.005. We show the corresponding algorithm of our ZO-RUDS defense in Alg. 1. Zhang *et al.* [81] directly applied ZO to the previous approach [62], with poor performance in the RGE optimization approach. However, we show in Table 1 in section 5.1, that after using our proposed RDUNet in ZO-RUDS defense mechanism, we achieve a huge increase of **35%** in certified accuracy compared to [81]. This proves that our proposed RDUNet type of architecture enables the model to learn fine-scale information while maintaining a low reconstruction error in comparison to previous custom-trained denoisers [62, 81].

---

#### Algorithm 1 ZO-RUDS Defense (RGE)

---

**Require:** Input  $x$ , noise  $\eta$ , smoothing parameter  $\xi$ , query directions  $q$ , dimensionality  $d$ , black-box predictor  $f$ , initial parameters  $\theta$  of RDUNet.

**Ensure:** Trained RDUNet  $D_\theta^u$

- 1:  $\hat{x} = D_\theta^u(x + \eta) = D_\theta^u(x^*)$ ,
  - 2: Calculate  $\mathcal{L}_{Tot}(f(x), f(\hat{x}))$  (Eq. 12),
  - 3: **for**  $k = 0$  to  $q - 1$  **do**
  - 4: Obtain a random direction vector  $u_k$  with Normal distribution  $N(\mu, \sigma)$ ,
  - 5: Calculate  $\hat{x}_q = \hat{x} + \xi \cdot u_k$ ,
  - 6: Calculate  $\mathcal{L}_{Tot}(f(x), f(\hat{x}_q))$  (Eq.12),
  - 7: Calculate gradient estimation using Eq.15,
  - 8: **end for**
- 

**ZO Autoencoder-based Robust UNet Denoised Smoothing (ZO-AE-RUDS).** We further pre-pend RDUNet followed by an encoder  $E_{\theta_e}$  and a decoder  $D_{\theta_d}$  to the black-box predictor for better performance on datasets like Tiny

Imagenet and STL-10 with large dimensionality. It ensures that ZO optimization can be carried out in a feature embedding space with low dimensions. However, the autoencoder can also lead to over-reduced features for these datasets leading to poor performance as in [81]. Thus, our ZO-AE-RUDS with RDUNet denoiser overcomes this disadvantage, and due to the ability of RDUNet to learn fine-scaled information leads to high performance. The objective function for our ZO-AE-RUDS defense is represented as,

$$\mathcal{L}_{Tot}^C(\theta) := \mathcal{L}_{Tot}(f(D_{\theta_d}(z)); z = E_{\theta_e}(D_\theta^u(x^*)), \quad (16)$$

where  $\mathcal{L}_{Tot}^C(\theta)$  represents that we optimize  $\mathcal{L}_{Tot}$  (Eq. 12) with CGE ZO optimization (C) [48]. We calculate gradient estimate of  $\mathcal{L}_{Tot}^C(\theta)$  as,

$$\hat{\nabla}_\theta \mathcal{L}_{Tot}^C(\theta) \approx \frac{dE_{\theta_e}(D_\theta^u(x^*))}{d\theta} \hat{\nabla}_z f(z)|_{z=E_{\theta_e}(D_\theta^u(x^*))}, \quad (17)$$

where  $z$  is the latent feature vector with reduced dimension  $d_r < d$ . This reduction in dimension makes the CGE ZO optimization approach feasible. Thus, we utilize CGE [46, 49] and calculate the gradient estimate of training objective function  $\mathcal{L}_{Tot}(\theta)$  as,

$$\hat{\nabla}_\theta \mathcal{L}_{Tot}^C(\theta) = \sum_{k=0}^{d-1} \left[ \frac{(\mathcal{L}_{Tot}(\theta + \xi e_k) - \mathcal{L}_{Tot}(\theta - \xi e_k))}{\xi} e_k \right], \quad (18)$$

where  $e^k \in \mathbb{R}^d$  is the  $k$ th elementary basis vector, with 1 at the  $k$ th coordinate and 0s elsewhere. We show the corresponding algorithm of our ZO-AE-RUDS defense using CGE optimization in Alg. 2.

---

#### Algorithm 2 ZO-AE-RUDS Defense (CGE)

---

**Require:** Input  $x$ , noise  $\eta$ , smoothing parameter  $\xi$ , query directions  $q$ , dimensionality  $d$ , black-box predictor  $f$ ,  $D_{\theta_d}$  decoder, initial parameters  $\theta$  of RDUNet, and  $\theta_e$  of white-box encoder  $E_{\theta_e}$

**Ensure:** Trained  $D_\theta^u + E_{\theta_e}$

- 1:  $z = E_{\theta_e}(D_\theta^u(x + \eta))$ ,
  - 2:  $\hat{x} = D_\theta^u(z)$ ,
  - 3: Calculate  $\mathcal{L}_{Tot}(f(x), f(\hat{x}))$  (Eq. 12),
  - 4: **for**  $k = 0$  to  $d - 1$  **do**
  - 5: Obtain a elementary basis direction vector  $e_k$ ,
  - 6: Calculate  $\hat{x}_q^+ = \hat{x} + \xi \cdot e_k$  and  $\hat{x}_q^- = \hat{x} - \xi \cdot e_k$ ,
  - 7: Calculate  $\mathcal{L}_{Tot}(f(x), f(E_{\theta_e}(\hat{x}_q^+)))$  (Eq. 12),
  - 8: Calculate  $\mathcal{L}_{Tot}(f(x), f(E_{\theta_e}(\hat{x}_q^-)))$  (Eq. 12),
  - 9: Calculate gradient estimation using Eq. 18,
  - 10: **end for**
- 

## 5. Experimental Settings

**Datasets and Models.** We evaluate the results on CIFAR-10 [40], CIFAR-100 [41], Tiny Imagenet [51] and STL-

10 [16] datasets for classification task. For image reconstruction, we focus on MNIST [43] dataset. We consider pre-trained models ResNet-110 for CIFAR-10 and ResNet-18 for STL-10. For CIFAR-100, we use Resnet-50 as the target classifier; for Tiny Imagenet dataset, we use ResNet-34. **Implementation Details.** We use learning rate  $10^{-4}$  and weight decay by 10 at every 100 epochs with total 600 epochs. We set the smoothing parameter  $\zeta = 0.005$  for a fair comparison with SOTA. We sample noise  $\eta$  with mean  $\mu = 0$  and variance  $\sigma^2 = 0.25$  from Normal distribution. We optimize ZO-RUDS with RGE (R) and ZO-AE-RUDS with CGE (C) optimization unless otherwise stated. **Evaluation Metrics.** We measure the robustification of our model using standard certified accuracy (SCA (%)) at  $l_2$ -radius ( $r$ ) = 0 and robust certified accuracy (RCA (%)) at  $r = \{0.25, 0.50, 0.75\}$ . Higher certified accuracy (CA) ensures that for a given  $r$ , more percentage of correctly predicted samples have certified radii larger than  $r$  [17].

### 5.1. Comparison with SOTA

We compare our proposed defense methods ZO-RUDS and ZO-AE-RUDS with previous certified defense approaches in white-box (W) and black-box (B) settings in Table 1. Our proposed defense methods ZO-RUDS and ZO-AE-RUDS with RDUNet comfortably outperform SOTA [81] by a large margin of **35%** and **9%** in RGE and CGE optimization approaches respectively. It consistently achieves higher certified robustness across different  $r$ . The high performance of ZO-RUDS over SOTA signifies that our method leads to an effective DS-oriented robust defense even without additional custom-trained autoencoder. We observe that our method provides better results in the black-box setting and better performance than RS [17] and DS [62], which defend the model in the white-box setting, thus proving the effectiveness of our approach.

### 5.2. Performance on Image Classification

**Performance on different number of queries.** We show the performance for other queries  $q = 20, 100$  for CIFAR-10 and  $q = 576$  for STL-10 dataset in Table 2. Our proposed robustification outperforms SOTA [81] on all these queries by a huge margin for SCA and RCA evaluation metrics at different  $l_2$  radii. We observe that [81] has poor performance for high-dimension images even after increasing the number of queries or using CGE optimization with autoencoder to decrease the variance caused by RGE optimization. This may happen due to two reasons; First, the bottleneck in the autoencoder architecture constrains the fine-scaled information necessary for reconstructing denoised images, and Second, the over-reduced feature dimension in high-dimension images could hamper the performance. Our proposed denoiser RDUNet with lateral connections between the encoder and decoder ensures better reconstruction

Method	Type	SCA	RCA ( $r$ )		
			0.25	0.50	0.75
RS [17]	W	76.22	61.20	43.23	25.67
DS (FO-DS) [62]	W	70.80	53.31	40.89	25.90
FO-AE-DS	W	75.92	60.54	46.45	32.19
DS [62]	B	74.89	44.56	18.20	14.39
ZO-DS (R) [81]	B	42.34	18.12	5.01	0.19
ZO-AE-DS (R) [81]	B	60.90	43.25	26.23	7.78
ZO-AE-DS (C) [81]	B	70.90	53.45	33.21	12.45
<b>ZO-RUDS (R)</b>	B	<b>77.89</b>	<b>58.92</b>	<b>38.31</b>	<b>21.93</b>
<b>ZO-AE-RUDS (R)</b>	B	<b>76.87</b>	<b>58.23</b>	<b>37.72</b>	<b>20.65</b>
<b>ZO-AE-RUDS (C)</b>	B	<b>79.87</b>	<b>61.32</b>	<b>42.90</b>	<b>23.21</b>

Table 1: Comparison with SOTA certified defense techniques in white-box (W) and black-box (B) settings on CIFAR-10 dataset. ‘R’ and ‘C’ are RGE and CGE optimization techniques. ‘q’=192.

CIFAR-10					
q	Model	SCA	RCA ( $r$ )		
			0.25	0.50	0.75
20	ZO-DS (R) [81]	18.56	3.88	0.53	0.26
	ZO-AE-DS (C) [81]	40.67	27.90	17.84	7.10
	<b>ZO-RUDS (R)</b>	<b>62.10</b>	<b>42.43</b>	<b>36.23</b>	<b>24.56</b>
	<b>ZO-AE-RUDS (C)</b>	<b>63.59</b>	<b>51.34</b>	<b>39.01</b>	<b>30.23</b>
100	ZO-DS (R) [81]	39.82	17.90	4.71	0.29
	ZO-AE-DS (C) [81]	54.32	40.90	23.98	9.35
	<b>ZO-RUDS (R)</b>	<b>74.60</b>	<b>58.71</b>	<b>39.56</b>	<b>27.82</b>
	<b>ZO-AE-RUDS (C)</b>	<b>76.34</b>	<b>62.46</b>	<b>44.29</b>	<b>30.22</b>
STL-10					
576	ZO-DS (R) [81]	37.59	21.23	8.67	2.56
	ZO-AE-DS (C) [81]	44.78	33.41	26.10	16.43
	<b>ZO-RUDS (R)</b>	<b>58.20</b>	<b>47.83</b>	<b>40.32</b>	<b>29.89</b>
	<b>ZO-AE-RUDS (C)</b>	<b>68.29</b>	<b>57.93</b>	<b>47.31</b>	<b>33.22</b>

Table 2: Comparison of our defense with previous ZO defense approaches. ‘q’ is the number of queries.

tion of denoised output, which ensures prediction with high certified accuracy. RDUNet decreases model variance as it consists of downsampling and upsampling layers in the encoding and decoding path, which makes the model invariant to changes in image dimensions and thus performs better for high dimensions as well. The lateral skip connections help the model learn fine-scale information, thus overcoming the disadvantage of auto-encoder constraining fine-scale information.

**Performance on low-dimension (CIFAR-10, CIFAR-100) and high-dimension (STL-10, Tiny Imagenet) classification datasets.** We compare our proposed defense methods ZO-RUDS (R) and ZO-AE-RUDS (C) with pre-

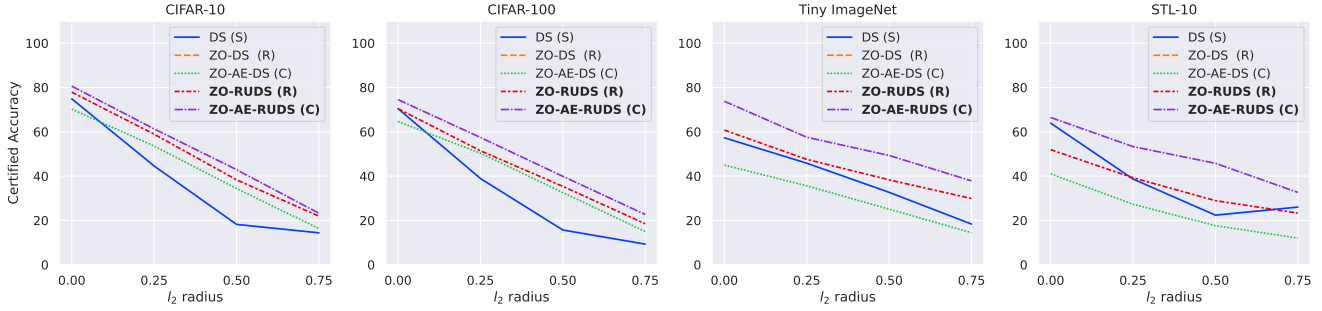


Figure 3: Comparison of Certified Accuracy on low-dimension (CIFAR-10, CIFAR-100) and high-dimension (STL-10 and Tiny Imagenet) datasets for different  $l_2$  radius at query  $q = 192$ . ‘R’- RGE and ‘C’- CGE ZO techniques.

vious black-box defense methods DS (S) [62], ZO-DS (R) [81] and ZO-AE-DS (C) [81] at various  $r$  for low and high-dimension classification datasets in Figure 3. Our proposed approaches ZO-RUDS and ZO-AE-RUDS beat the SOTA [81] by a large margin of **30.21%** and **8.87%** in RGE, and CGE optimization approaches respectively for CIFAR-100 dataset. It outperforms SOTA by a huge margin for all other radii as well. We show that unlike [81], which gives better performance only for the CGE optimization approach after appending autoencoder in ZO-AE-RUDS, our proposed RDUNet denoiser when appended to predictor performs better for both RGE and CGE optimization approaches. We observe that SOTA [81] fails to perform even after the addition of an autoencoder to the network for high-dimension Tiny Imagenet and STL-10 datasets. Our defense methods ZO-RUDS and ZO-AE-RUDS beats SOTA [81] by a huge margin of **24.81%** and **25.84%** respectively for Tiny Imagenet dataset. Similar observations can be made for CIFAR-10 and STL-10 datasets at different certified radii, as shown in Figure 3.

### 5.3. Performance on Image Reconstruction

Previous works [4, 58, 73] show that image reconstruction networks are vulnerable to adversarial attacks like PGD attacks [53]. We compare our proposed defense methods

ZO-RUDS and ZO-AE-RUDS with previous white-box and black-box defense methods in Table 3. We follow the settings of [81] and aim to recover the original sample using a pre-trained reconstruction network [58] under adversarial perturbations generated by a 40-step  $l_2$  PGD attack under  $\|\delta\|_2 = \{0, 1, 2, 3, 4\}$ . We use root mean square error (RMSE) and structural similarity (SSIM) [31] to find the similarity between the original and reconstructed image. We observe that our method beats SOTA [81] with low RMSE and high SSIM scores for all the values of  $\|\delta\|_2$ . Our defense beats FO defense methods as well as the vanilla model, proving the robustness provided by our method for the reconstruction task. We observe that at high values of  $\|\delta\|_2$  perturbation the performance of vanilla model [58] decreases drastically.

Loss	SCA	RCA ( $r$ )		
		0.25	0.50	0.75
$\mathcal{L}_{CE}$	72.67	54.90	36.01	17.03
$\mathcal{L}_{CE} + \mathcal{L}_{CS}$	73.21	56.04	36.45	18.79
$\mathcal{L}_{CE} + \mathcal{L}_{CS} + \mathcal{L}_{MMD}$	<b>79.87</b>	<b>61.32</b>	<b>42.90</b>	<b>23.21</b>

Table 4: Effect of loss functions on our proposed (ZO-AE-RUDS) for  $q = 192$ . Dataset is CIFAR-10.

Method	$\ \delta\ _2 = 0$		$\ \delta\ _2 = 1$		$\ \delta\ _2 = 2$		$\ \delta\ _2 = 3$		$\ \delta\ _2 = 4$	
	RMSE	SSIM	RMSE	SSIM	RMSE	SSIM	RMSE	SSIM	RMSE	SSIM
Vanilla [58]	0.1213	0.7934	0.3251	0.4367	0.4629	0.1468	0.6129	0.04945	0.5976	0.0168
FO-DS [62]	0.1596	0.7415	0.1692	0.6934	0.2182	0.5421	0.2698	0.3956	0.3245	0.3178
FO-AE-DS [81]	0.1475	0.7594	0.1782	0.7025	0.2182	0.5421	0.2693	0.4163	0.3176	0.3293
ZO-DS (R) [81]	0.1892	0.5345	0.2267	0.4634	0.2634	0.3689	0.3092	0.2792	0.3482	0.2177
ZO-AE-DS (C) [81]	0.1398	0.6894	0.1634	0.7099	0.2126	0.5472	0.2689	0.4188	0.3367	0.3294
<b>ZO-RUDS (R)</b>	<b>0.1232</b>	<b>0.7924</b>	<b>0.1465</b>	<b>0.7991</b>	<b>0.2053</b>	<b>0.5966</b>	<b>0.2380</b>	<b>0.4591</b>	<b>0.3082</b>	<b>0.3811</b>
<b>ZO-AE-RUDS (C)</b>	<b>0.1219</b>	<b>0.7926</b>	<b>0.1392</b>	<b>0.8346</b>	<b>0.1872</b>	<b>0.6648</b>	<b>0.2174</b>	<b>0.6102</b>	<b>0.2679</b>	<b>0.5236</b>

Table 3: Performance comparison of image reconstruction task on MNIST dataset. ( $q = 192$ )



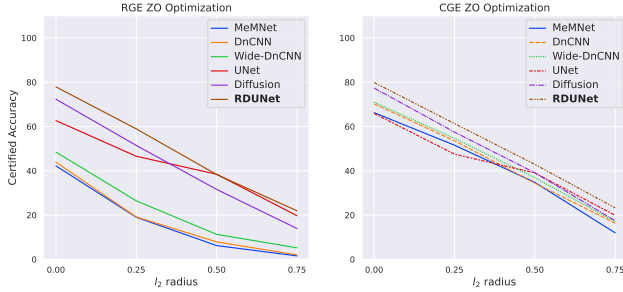


Figure 4: Effect of different denoisers on our RGE and CGE ZO optimization-based defense approaches for different  $l_2$ -radii at  $q=192$ . Dataset is CIFAR-10.

Training Strategy	SCA	RCA ( $l_2$ -radius)		
		0.25	0.50	0.75
$(D_\theta^u)_{finetune}$	67.52	53.44	29.56	12.87
$(D_\theta^u)_{scratch}$	<b>79.87</b>	<b>61.32</b>	<b>42.90</b>	<b>23.21</b>

Table 5: Effect of RDUNet training strategies on ZO-AE-RUDS for  $q = 192$ . Dataset is CIFAR-10.

#### 5.4. Ablation Study

We show the effect of loss functions and different denoiser architectures in our proposed defense mechanism.

**Effect of various denoisers.** We compare our proposed robust denoiser RDUNet with previous denoisers MemNet [66], DnCNN [79], wide-DnCNN [79], UNet [59] and Diffusion [30] in Figure 4. We show that after appending denoiser DnCNN as proposed in [62, 81] with 17 layers primarily including Conv+BN+ReLU layers and wide-DnCNN with 128 deep layers to the black-box model in the RGE optimization leads to poor performance. We observe that appending these denoisers to the autoencoder architecture in the CGE optimization improves the robustification of the model to some extent. We show that the diffusion model gives comparatively better performance than other denoisers. However, RDUNet gives better performance than diffusion models. It may happen due to multiple noise addition, which makes ZO optimization of the diffusion model unstable. These results conclude that our proposed RDUNet provides robustness to a black-box model against adversarial perturbations.

**Effect of Loss Functions.** We show in Table 4, the effect of cosine similarity loss  $\mathcal{L}_{CS}$  at the sample level and MMD loss  $\mathcal{L}_{MMD}$  between the probability distributions of the original samples and denoised output. We observe in Table 4 that after applying  $\mathcal{L}_{CS}$  in addition to cross-entropy loss, our model’s performance increases by 1% and using  $\mathcal{L}_{MMD}$  the performance increase by approximately 6%. This shows that bringing closer the features of the origi-

nal sample and denoised output at the instance and domain level increase the robustness of the black-box model.

**Effect of training strategies.** We show the effect of our training schemes (over RDUNet) on ZO-AE-RUDS across different  $r$  in Table 5.  $(D_\theta^u)_{finetune}$  represents pre-training RDUNet and then fine-tuning it in our defense method, and  $(D_\theta^u)_{scratch}$  is training RDUNet from scratch. We show that training from scratch gives better performance than pre-training and fine-tuning RDUNet. We observe during training that  $(D_\theta^u)_{finetune}$  achieves very high performance at the initial training stage; however, it does not improve as training progresses. Pre-training the denoiser causes the optimization to get stuck at a local optima leading to decreased performance.

## 6. Conclusion

In this work, we study the problem of certified black-box defense, aiming to robustify the black-box model with access only to input queries and output feedback. First, we proposed two novel defense mechanisms, ZO-RUDS and ZO-AE-RUDS, which substantially enhance the defense and optimization performance by reducing the variance of ZO gradient estimates. Second, we proposed a novel robust denoiser RDUNet that provides a scalable defense by directly integrating denoised smoothing with RGE ZO optimization, which was not feasible in previous works. We show that RDUNet gives high performance by further appending autoencoder (AE) as in ZO-AE-RUDS defense. Lastly, we proposed an objective function with MMD loss, bringing the distribution of denoised output closer to clean data. Our elaborate experiments demonstrate that ZO-RUDS and ZO-AE-RUDS achieve SOTA-certified defense performance on classification and reconstruction tasks.

## References

- [1] Sravanti Addepalli, Vivek BS, Arya Baburaj, Gaurang Sriramanan, and R Venkatesh Babu. Towards achieving adversarial robustness by enforcing feature consistency across bit planes. In *Proceedings of the CVPR*, pages 1020–1029, 2020.
- [2] Sravanti Addepalli, Samyak Jain, Gaurang Sriramanan, and R Venkatesh Babu. Boosting adversarial robustness using feature level stochastic smoothing. In *Proceedings of the CVPR*, pages 93–102, 2021.
- [3] Shun-ichi Amari. Backpropagation and stochastic gradient descent method. *Neurocomputing*, 5(4-5):185–196, 1993.
- [4] Vegard Antun, Francesco Renna, Clarice Poon, Ben Adcock, and Anders C Hansen. On instabilities of deep learning in image reconstruction and the potential costs of ai. *PNAS*, 117(48):30088–30095, 2020.
- [5] Anish Athalye, Nicholas Carlini, and David Wagner. Obfuscated gradients give a false sense of security: Circumventing defenses to adversarial examples. In *ICML*, pages 274–283. PMLR, 2018.

- [6] Anish Athalye, Logan Engstrom, Andrew Ilyas, and Kevin Kwok. Synthesizing robust adversarial examples. In *ICML*, pages 284–293. PMLR, 2018.
- [7] Tom B Brown, Dandelion Mané, Aurko Roy, Martín Abadi, and Justin Gilmer. Adversarial patch. *arXiv preprint arXiv:1712.09665*, 2017.
- [8] Rudy R Bunel, Ilker Turkaslan, Philip Torr, Pushmeet Kohli, and Pawan K Mudigonda. A unified view of piecewise linear neural network verification. *Advances in Neural Information Processing Systems*, 31, 2018.
- [9] HanQin Cai, Yuchen Lou, Daniel McKenzie, and Wotao Yin. A zeroth-order block coordinate descent algorithm for huge-scale black-box optimization. In *ICML*, pages 1193–1203. PMLR, 2021.
- [10] HanQin Cai, Daniel Mckenzie, Wotao Yin, and Zhenliang Zhang. Zeroth-order regularized optimization (zoro): Approximately sparse gradients and adaptive sampling. *SIAM Journal on Optimization*, 32(2):687–714, 2022.
- [11] Nicholas Carlini and David Wagner. Towards evaluating the robustness of neural networks. In *2017 SP*, pages 39–57. Ieee, 2017.
- [12] Yair Carmon, Aditi Raghunathan, Ludwig Schmidt, John C Duchi, and Percy S Liang. Unlabeled data improves adversarial robustness. *Adv. neural inf. process. syst.*, 32, 2019.
- [13] Alvin Chan, Yi Tay, Yew Soon Ong, and Jie Fu. Jacobian adversarially regularized networks for robustness. *arXiv preprint arXiv:1912.10185*, 2019.
- [14] Pin-Yu Chen, Huan Zhang, Yash Sharma, Jinfeng Yi, and Cho-Jui Hsieh. Zoo: Zeroth order optimization based black-box attacks to deep neural networks without training substitute models. In *Proceedings of the 10th ACM AISec*, pages 15–26, 2017.
- [15] Zhen Cheng, Fei Zhu, Xu-Yao Zhang, and Cheng-Lin Liu. Adversarial training with distribution normalization and margin balance. *Pattern Recognition*, 136:109182, 2023.
- [16] Adam Coates, Andrew Y Ng, and Honglak Lee. The stl-10 dataset. <https://cs.stanford.edu/acoates/stl10/>, 2011.
- [17] Jeremy Cohen, Elan Rosenfeld, and Zico Kolter. Certified adversarial robustness via randomized smoothing. In *ICML*, pages 1310–1320. PMLR, 2019.
- [18] Francesco Croce and Matthias Hein. Reliable evaluation of adversarial robustness with an ensemble of diverse parameter-free attacks. In *Proceedings of the 37th ICML, ICML’20*. JMLR.org, 2020.
- [19] Jiequan Cui, Shu Liu, Liwei Wang, and Jiaya Jia. Learnable boundary guided adversarial training. In *Proceedings of the ICCV*, pages 15721–15730, 2021.
- [20] Vincent Dumoulin, Francesco Visin, Marc A. G. Mazzeo, Matteo Matteucci, and Yann N. Dauphin. A guide to convolution arithmetic for deep learning. *CoRR*, abs/1603.07285, 2016.
- [21] Souradeep Dutta, Susmit Jha, Sriram Sanakaranarayanan, and Ashish Tiwari. Output range analysis for deep neural networks. *arXiv preprint arXiv:1709.09130*, 2017.
- [22] Ilham A Elaalami, Sunday O Olatunji, and Rachid M Zagrouba. At-bod: An adversarial attack on fool dnn-based blackbox object detection models. *Applied Sciences*, 12(4):2003, 2022.
- [23] Kevin Eykholt, Ivan Evtimov, Earlence Fernandes, Bo Li, Amir Rahmati, Chaowei Xiao, Atul Prakash, Tadayoshi Kohno, and Dawn Song. Robust physical-world attacks on deep learning visual classification. In *Proceedings of the CVPR*, pages 1625–1634, 2018.
- [24] Joachim Folz, Sebastian Palacio, Joern Hees, and Andreas Dengel. Adversarial defense based on structure-to-signal autoencoders. In *2020 WACV*, pages 3568–3577. IEEE, 2020.
- [25] Matt Fredrikson, Somesh Jha, and Thomas Ristenpart. Model inversion attacks that exploit confidence information and basic countermeasures. In *Proceedings of the 22nd ACM CCS*, pages 1322–1333, 2015.
- [26] Ian J Goodfellow, Jonathon Shlens, and Christian Szegedy. Explaining and harnessing adversarial examples. *arXiv preprint arXiv:1412.6572*, 2014.
- [27] Arthur Gretton, Karsten M Borgwardt, Malte J Rasch, Bernhard Schölkopf, and Alexander Smola. A kernel two-sample test. *The Journal of Machine Learning Research*, 13(1):723–773, 2012.
- [28] Rahul Gupta, Robert Stanforth, and Philipp Hennig. Verifiable robustness of neural networks with contractive activation functions. In *Proceedings of the 38th ICML*, pages 3774–3784. PMLR, 2021.
- [29] Geoffrey Hinton, Oriol Vinyals, Jeff Dean, et al. Distilling the knowledge in a neural network. *arXiv preprint arXiv:1503.02531*, 2(7), 2015.
- [30] Jonathan Ho, Ajay Jain, and Pieter Abbeel. Denoising diffusion probabilistic models. *Advances in Neural Information Processing Systems*, 33:6840–6851, 2020.
- [31] Alain Hore and Djemel Ziou. Image quality metrics: Psnr vs. ssim. In *2010 20th ICPR*, pages 2366–2369. IEEE, 2010.
- [32] Zhichao Huang and Tong Zhang. Black-box adversarial attack with transferable model-based embedding. In *ICLR*, 2020.
- [33] Mubashir Hussain, Deepika Koundal, and Jatinder Manhas. Deep learning-based diagnosis of disc degenerative diseases using mri: A comprehensive review. *Computers and Electrical Engineering*, 105:108524, 2023.
- [34] Andrew Ilyas, Logan Engstrom, Anish Athalye, and Jessy Lin. Black-box adversarial attacks with limited queries and information. In *ICML*, pages 2137–2146. PMLR, 2018.
- [35] Andrew Ilyas, Logan Engstrom, and Aleksander Madry. Prior convictions: Black-box adversarial attacks with bandits and priors. *arXiv preprint arXiv:1807.07978*, 2018.
- [36] Sergey Ioffe and Christian Szegedy. Batch normalization: Accelerating deep network training by reducing internal covariate shift. In *ICML*, pages 448–456. PMLR, 2015.
- [37] Chaitanya K. Joshi, Chaoqi Yang, and Suhang Wang. Certified robustness of graph neural networks against adversarial attacks. In *Proceedings of the AIES*, volume 36, pages 4415–4422, 2022.
- [38] Guy Katz, Clark Barrett, David L Dill, Kyle Julian, and Mykel J Kochenderfer. Reluplex: An efficient smt solver for verifying deep neural networks. In *CAV*, pages 97–117. Springer, 2017.
- [39] Guy Katz, Clark Barrett, David L. Dill, Kyle Julian, and Mykel J. Kochenderfer. Formal verification of neural net-

- works: From verification of robustness to certificates. *IEEE Trans Neural Netw Learn Syst*, 2022.
- [40] Alex Krizhevsky and Geoffrey Hinton. Cifar-10 (canadian institute for advanced research). <https://www.cs.toronto.edu/kriz/cifar.html>, 2009.
- [41] Alex Krizhevsky and Geoffrey Hinton. Cifar-100 (canadian institute for advanced research). <https://www.cs.toronto.edu/kriz/cifar.html>, 2009.
- [42] Alex Krizhevsky, Ilya Sutskever, and Geoffrey E Hinton. Imagenet classification with deep convolutional neural networks. In *Adv. neural inf. process. syst.*, pages 1097–1105, 2012.
- [43] Yann LeCun, Corinna Cortes, and CJ Burges. The mnist database. <http://yann.lecun.com/exdb/mnist/>, 1998.
- [44] Mathias Lecuyer, Vaggelis Atlidakis, Roxana Geambasu, Daniel Hsu, and Suman Jana. Certified robustness to adversarial examples with differential privacy. In *2019 SP*, pages 656–672. IEEE, 2019.
- [45] Bai Li, Changyou Chen, Wenlin Wang, and Lawrence Carin. Certified adversarial robustness with additive noise. *Adv. neural inf. process. syst.*, 32, 2019.
- [46] Xiangru Lian, Huan Zhang, Cho-Jui Hsieh, Yijun Huang, and Ji Liu. A comprehensive linear speedup analysis for asynchronous stochastic parallel optimization from zeroth-order to first-order. *Adv. neural inf. process. syst.*, 29, 2016.
- [47] Sijia Liu, Pin-Yu Chen, Xiaojie Chen, and Mingyi Hong. signsgd via zeroth-order oracle. In *ICLR*, 2019.
- [48] Sijia Liu, Pin-Yu Chen, Bhavya Kailkhura, Gaoyuan Zhang, Alfred O Hero III, and Pramod K Varshney. A primer on zeroth-order optimization in signal processing and machine learning: Principals, recent advances, and applications. *IEEE Signal Processing Magazine*, 37(5):43–54, 2020.
- [49] Sijia Liu, Bhavya Kailkhura, Pin-Yu Chen, Paishun Ting, Shiyu Chang, and Lisa Amini. Zeroth-order stochastic variance reduction for nonconvex optimization. *Adv. neural inf. process. syst.*, 31, 2018.
- [50] Sijia Liu, Si Lu, Xiaojie Chen, Yisen Feng, Ke Xu, Abdullah Al-Dujaili, Mingyi Hong, and Una-May O’Reilly. Min-max optimization without gradients: Convergence and applications to adversarial ml. In *ICML*, 2020a.
- [51] Xiaojie Liu, Yunchao Wang, Ting Liu, and Zhang Zhang. Tiny imagenet visual recognition challenge. In *ACM Multimedia*, pages 909–910. ACM, 2017.
- [52] Xingjun Ma, Yang Liu, James Bailey, and Honghui Shi. Towards certified robustness for deep neural networks with lipschitz continuous activations. *IEEE Trans Neural Netw Learn Syst*, 32(2):458–470, 2021.
- [53] Aleksander Madry, Aleksandar Makelov, Ludwig Schmidt, Dimitris Tsipras, and Adrian Vladu. Towards deep learning models resistant to adversarial attacks. *arXiv preprint arXiv:1706.06083*, 2017.
- [54] Djebril Mekhazni, Amran Bhuiyan, George Ekladios, and Eric Granger. Unsupervised domain adaptation in the dissimilarity space for person re-identification. In *ECCV*, pages 159–174. Springer, 2020.
- [55] Nicolas Papernot, Patrick McDaniel, Somesh Jha, Matt Fredrikson, Z Berkay Celik, and Ananthram Swami. The limitations of deep learning in adversarial settings. In *2016 EuroS&P*, pages 372–387. IEEE, 2016.
- [56] Nicolas Papernot, Patrick McDaniel, Xi Wu, Somesh Jha, and Ananthram Swami. Distillation as a defense to adversarial perturbations against deep neural networks. In *2016 SP*, pages 582–597. IEEE, 2016.
- [57] Aditi Raghunathan, Jacob Steinhardt, and Percy Liang. Certified defenses against adversarial examples. *arXiv preprint arXiv:1801.09344*, 2018.
- [58] Ankit Raj, Yoram Bresler, and Bo Li. Improving robustness of deep-learning-based image reconstruction. In *ICML*, pages 7932–7942. PMLR, 2020.
- [59] Olaf Ronneberger, Philipp Fischer, and Thomas Brox. U-net: Convolutional networks for biomedical image segmentation. In *Medical Image Computing and Computer-Assisted Intervention—MICCAI 2015: 18th International Conference, Munich, Germany, October 5-9, 2015, Proceedings, Part III 18*, pages 234–241. Springer, 2015.
- [60] Hadi Salman, Saachi Jain, Eric Wong, and Aleksander Madry. Certified patch robustness via smoothed vision transformers. In *Proceedings of the CVPR*, pages 15137–15147, 2022.
- [61] Hadi Salman, Jerry Li, Ilya Razenshteyn, Pengchuan Zhang, Huan Zhang, Sebastien Bubeck, and Greg Yang. Provably robust deep learning via adversarially trained smoothed classifiers. *Adv. neural inf. process. syst.*, 32, 2019.
- [62] Hadi Salman, Mingjie Sun, Greg Yang, Ashish Kapoor, and J Zico Kolter. Denoised smoothing: A provable defense for pretrained classifiers. *Adv. neural inf. process. syst.*, 33:21945–21957, 2020.
- [63] Vikash Sehwal, Saeed Mahloujifar, Tinashe Handina, Sihui Dai, Chong Xiang, Mung Chiang, and Prateek Mittal. Robust learning meets generative models: Can proxy distributions improve adversarial robustness? *arXiv preprint arXiv:2104.09425*, 2021.
- [64] Abhisar Sinha, Swati Purohit Joshi, Purnendu Sekhar Das, Soumya Jana, and Rahuldeb Sarkar. An ml prediction model based on clinical parameters and automated ct scan features for covid-19 patients. *Scientific Reports*, 12(1):11255, 2022.
- [65] Christian Szegedy, Wojciech Zaremba, Ilya Sutskever, Joan Bruna, Dumitru Erhan, Ian Goodfellow, and Rob Fergus. Intriguing properties of neural networks. *arXiv preprint arXiv:1312.6199*, 2013.
- [66] Ying Tai, Jian Yang, Xiaoming Liu, and Chunyan Xu. Memnet: A persistent memory network for image restoration. In *Proceedings of the ICCV*, pages 4539–4547, 2017.
- [67] Vincent Tjeng, Kai Xiao, and Russ Tedrake. Evaluating robustness of neural networks with mixed integer programming. *arXiv preprint arXiv:1711.07356*, 2017.
- [68] Chun-Chen Tu, Paishun Ting, Pin-Yu Chen, Sijia Liu, Huan Zhang, Jinfeng Yi, Cho-Jui Hsieh, and Shin-Ming Cheng. Autozoom: Autoencoder-based zeroth order optimization method for attacking black-box neural networks. In *Proceedings of the AIES*, volume 33, pages 742–749, 2019.
- [69] Jonathan Uesato, Brendan O’Donoghue, Pushmeet Kohli, and Aaron van den Oord. Adversarial risk and the dangers of evaluating against weak attacks. In *Proceedings of the PMLR*, pages 5025–5034, 2018.

- [70] Hongjun Wang and Yisen Wang. Self-ensemble adversarial training for improved robustness. *ICLR*, 2022.
- [71] Jiefei Wei, Luyan Yao, and Qinggang Meng. Self-adaptive logit balancing for deep neural network robustness: Defence and detection of adversarial attacks. *Neurocomputing*, 2023.
- [72] Xingxing Wei, Ying Guo, Jie Yu, and Bo Zhang. Simultaneously optimizing perturbations and positions for black-box adversarial patch attacks. *IEEE Trans. Pattern Anal. Mach. Intell.*, 2022.
- [73] Adva Wolf. Making medical image reconstruction adversarially robust.
- [74] Eric Wong and Zico Kolter. Provable defenses against adversarial examples via the convex outer adversarial polytope. In *ICML*, pages 5286–5295. PMLR, 2018.
- [75] Jun Yan, Huilin Yin, Xiaoyang Deng, Ziming Zhao, Wancheng Ge, Hao Zhang, and Gerhard Rigoll. Wavelet regularization benefits adversarial training. *arXiv preprint arXiv:2206.03727*, 2022.
- [76] Fei Yin, Yong Zhang, Baoyuan Wu, Yan Feng, Jingyi Zhang, Yanbo Fan, and Yujiu Yang. Generalizable black-box adversarial attack with meta learning. *IEEE Trans. Pattern Anal. Mach. Intell.*, 2023.
- [77] Huan Zhang, Tsui-Wei Weng, Pin-Yu Chen, Cho-Jui Hsieh, and Luca Daniel. Efficient neural network robustness certification with general activation functions. *Adv. neural inf. process. syst.*, 31, 2018.
- [78] Hongyang Zhang, Yaodong Yu, Jiantao Jiao, Eric Xing, Laurent El Ghaoui, and Michael Jordan. Theoretically principled trade-off between robustness and accuracy. In *ICML*, pages 7472–7482. PMLR, 2019.
- [79] Kai Zhang, Wangmeng Zuo, Yunjin Chen, Deyu Meng, and Lei Zhang. Beyond a gaussian denoiser: Residual learning of deep cnn for image denoising. *IEEE transactions on image processing*, 26(7):3142–3155, 2017.
- [80] Wen Zhang and Dongrui Wu. Discriminative joint probability maximum mean discrepancy (djp-mmd) for domain adaptation. In *2020 IJCNN*, pages 1–8. IEEE, 2020.
- [81] Yimeng Zhang, Yuguang Yao, Jinghan Jia, Jinfeng Yi, Mingyi Hong, Shiyu Chang, and Sijia Liu. How to robustify black-box ml models? a zeroth-order optimization perspective. *ICLR*, 2022.
- [82] Zijun Zhang. Improved adam optimizer for deep neural networks. In *2018 IEEE/ACM 26th IWQoS*, pages 1–2. Ieee, 2018.
- [83] Zhun Zhong, Liang Zheng, Zhedong Zheng, Shaozi Li, and Yi Yang. Camera style adaptation for person re-identification. In *Proceedings of the CVPR*, pages 5157–5166, 2018.